Accepted Manuscript

New Atglistatin closely related analogues: synthesis and structure-activity relationship towards adipose triglyceride lipase inhibition

Pierre-Philippe Roy, Kenneth D'Souza, Miroslava Cuperlovic-Culf, Petra C. Kienesberger, Mohamed Touaibia

PII: S0223-5234(16)30305-1

DOI: 10.1016/j.ejmech.2016.04.021

Reference: EJMECH 8536

To appear in: *European Journal of Medicinal Chemistry*

Received Date: 20 February 2016

Revised Date: 6 April 2016

Accepted Date: 7 April 2016

Please cite this article as: P.-P. Roy, K. D'Souza, M. Cuperlovic-Culf, P.C. Kienesberger, M. Touaibia, New Atglistatin closely related analogues: synthesis and structure-activity relationship towards adipose triglyceride lipase inhibition, *European Journal of Medicinal Chemistry* (2016), doi: 10.1016/j.ejmech.2016.04.021.

Graphical abstract

New Atglistatin closely related analogues: synthesis and structure-activity relationship towards adipose triglyceride lipase inhibition

Pierre-Philippe Roy, Kenneth D'Souza, Miroslava Cuperlovic-Culf, Petra C. Kienesberger and Mohamed Touaibia*.

New Atglistatin closely related analogues were synthesized. Their effects on adipose triglyceride lipase activities were evaluated.

Series A
R^1 or R^2 = $NHCON(CH_3)_2$ or H; R^3 or R^4 = $N(CH_3)_2$ or H
Series B
R^1 or R^2 = $N(CH_3)_2$ or H; R^3 or R^4 = $N(CH_3)_2$ or H
Series C
R^1 or R^2 = $NHCON(CH_3)_2$ or H; R^3 or R^4 = $NHCON(CH_3)_2$ or H

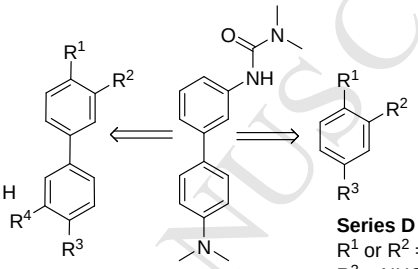

Aglistatin (**1**)

Series D
R^1 or R^2 = $NHCO_2N(CH_3)_2$ or $N(CH_3)_2$
R^3 = $NHCON(CH_3)_2$ or $N(CH_3)_2$

New Atglistatin closely related analogues: synthesis and structure-activity relationship towards adipose triglyceride lipase inhibition

Pierre-Philippe Roy[1], Kenneth D'Souza[2], Miroslava Cuperlovic-Culf[3], Petra C. Kienesberger[2] and Mohamed Touaibia[1*]

[1]Department of Chemistry and Biochemistry, Université de Moncton, Moncton, New Brunswick, Canada E1A 3E9.
[2]Department of Biochemistry and Molecular Biology, Dalhousie University, Saint John, NB E2L 4L5, Canada.
[3]National Research Council of Canada, 1200 Montreal Road; Ottawa, ON, Canada

[*] To whom correspondence should be sent at the above address.
Tel: (506) 858-4493; Fax: (506) 858-4541

Email: mohamed.touaibia@umoncton.ca

Abstract

Adipose Triglyceride Lipase (ATGL) performs the first and rate-limiting step in lipolysis by hydrolyzing triacylglycerols stored in lipid droplets to diacylglycerols. By mediating lipolysis in adipose and non-adipose tissues, ATGL is a major regulator of overall energy metabolism and plasma lipid levels. Since chronically high levels of plasma lipids are linked to metabolic disorders including insulin resistance and type 2 diabetes, ATGL is an interesting therapeutic target. In the present study, fourteen closely related analogues of Atglistatin (**1**), a newly discovered ATGL inhibitor, were synthesized, and their ATGL inhibitory activity was evaluated. The effect of these analogues on lipolysis in 3T3-L1 adipocytes clearly shows that inhibition of the enzyme by Atglistatin (**1**) is due to the presence of the carbamate and *N,N*-dimethyl moieties on the biaryl central core at *meta* and *para* position, respectively. Mono carbamate-substituted analogue **C2**, in which the carbamate group was in the *meta* position as in Atglistatin (**1**), showed slight inhibition. Low dipole moment of Atglistatin (**1**) compared to the synthesized analogues possibly explains the lower inhibitory activities.

Keywords: Adipose Triglyceride Lipase (ATGL), Atglistatin, Inhibitors, Structure–activity relationship, Lipolysis, Adipocytes

1. Introduction

Obesity is associated with increased adipose tissue lipolysis, which is believed to contribute to obesity-related comorbidities including insulin resistance and type 2 diabetes [1]. In light of the worldwide obesity pandemic, there has been a growing interest in developing drugs to control adipose tissue lipolysis and circulating lipid levels. During obesity, chronically elevated levels of plasma fatty acids (FA) can cause an accumulation of intracellular lipids in non-adipose tissues such as liver, skeletal muscle and heart, producing a lipotoxic environment that can trigger insulin resistance, inflammation [2,3] and lipoapoptosis [4]. Besides playing an important role in obesity and obesity comorbidities, adipose tissue lipolysis has also been shown to contribute to cancer cachexia, a metabolic disorder which is characterized by the extensive loss of adipose tissue and skeletal muscle mass and increases morbidity and mortality in cancer patients [5,6]. Hence, adipose tissue lipolysis could possibly be targeted for the treatment of cachexia by protecting from excessive adipose tissue depletion in cancer patients [6].

The release of FA from adipose tissue into the blood stream requires three lipases, which sequentially break down triacylglycerol stores within lipid droplets: Adipose Triglyceride Lipase (ATGL), Hormone-Sensitive Lipase (HSL) and Monoglyceride Lipase (MGL)[7,8]. ATGL initiates lipolysis, hydrolyzing triacylglycerol to generate FA and diacylglycerol [9]. The diacylglycerol is then hydrolyzed by HSL, producing a FA and monoacylglycerol, which can be further hydrolyzed by MGL [7], completing the lipolytic cascade. Since ATGL performs the first and rate-limiting step in lipolysis, this enzyme is an interesting target for the design of lipolysis inhibitors with therapeutic potential.

Recently, Mayer et al. [10] have developed a specific inhibitor of ATGL named Atglistatin (**1**, Figure 1). Atglistatin (**1**) inhibits the activity of ATGL (IC_{50} = 0.7 µM) in a competitive mechanism [10]. Few other ATGL inhibitors have also been developed, such as a peptide derived from G_0/G_1 Switch Gene 2 protein [11] and a hydrazone base compound [12].

While the inhibition of ATGL shows promise in the treatement of metabolic diseases such as obesity-induced insulin resistance and type-2 diabetes [13,14] as well as cachexia [6], chronic ATGL deficiency can cause cardiomyopathy in mice and humans, leading to premature death through severe accumulation of triacylglycerols and impairment of mitochondrial function in cardiac tissues [15,16,17]. However, inhibition of ATGL does not appear to cause increased

cardiac triacylglycerol accumulation as ATGL inhibitors such as Atglistatin (**1**) do not accumulate in cardiac tissues [10].

Since ATGL has not been crystallized the developpement of new ATGL inhibitors must be done by the traditional struture-activity relationship study (SAR). Studying the relationship between the structure of a known inhibitor and its capacity to inhibit the target enzyme leads not only to the optimization of said inhibitor, but also brings new insight into the enzyme structure.

In this paper we describe the design, synthesis, and biological activity of fourteen novel analogues closely related to Atglistatin (**1**). These compounds were evaluated for their ability to inhibit isoproterenol-stimulated lipolysis in 3T3-L1 adipocytes as a readout of their potential to inhibit ATGL in adipose tissue. Our work represents the first systematic structure-activity relationship study of such Atglistatin (**1**) analogues.

2. Results and discussion

2.1. Chemistry

To investigate the structure-activity relationship of Atglistatin (**1**) as an ATGL inhibitor, closely related analogues were synthesized. We examined the importance of the carbamate and the *N*,*N*-dimethyl moieties by either removing them or by interchanging the carbamate by the *N*,*N*-dimethyl and vice versa (Figure 1). Then, the effect of the position of these groups was investigated by the synthesis of analogues with the carbamate and the *N*,*N*-dimethyl moieties in the *meta* or *para* positions. The synthesis of analogues having an aryl central core allowed us to investigate whether the biaryl core of Atglistatin (**1**) is necessary for ATGL inhibition.

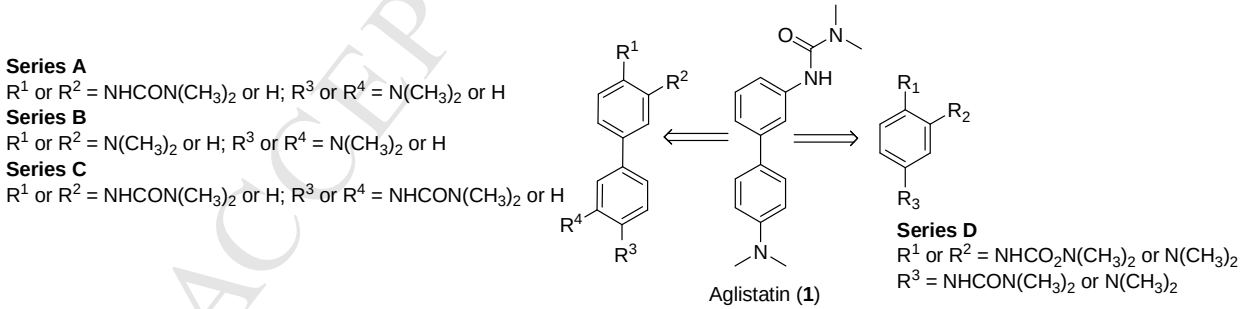

Figure 1. Structural analogues based on (**1**) synthesized in this work.

Analogues of Aglistatin (**1**) **A1-D3** (Figure 1) were obtained in moderate to good yields through Suzuki-Miyaura [18] cross coupling or copper(I) catalyzed homocoupling conditions [19], catalytic hydrogenation, *N*-methylation, and Schotten-Baumann condensation.

To investigate the necessity of the 3 and 4' substitution of the biaryl central core of Aglistatin (**1**), analogues with the carbamate and the *N*,*N*-dimethyl moieties at 3 and 4' positions were synthesized (**A1**-**A3**, Scheme 1). Intermediates **6**, **7**, and **8** were synthesized starting from *meta* and *para* nitroboronic acids (**2**, **3**) and bromo-*N*,*N*-dimethylaniline (**4**, **5**) under Suzuki-Miyaura [18] cross coupling conditions. Corresponding amines **9**, **10**, and **11** were then obtained in a quantitative yield after a catalytic hydrogenation over Pd/C. The final products **A1**, **A2**, and **A3** were obtained from amines **9**, **10**, and **11** through Schotten-Baumann condensation conditions with dimethylcarbamoyl chloride (Scheme 1).

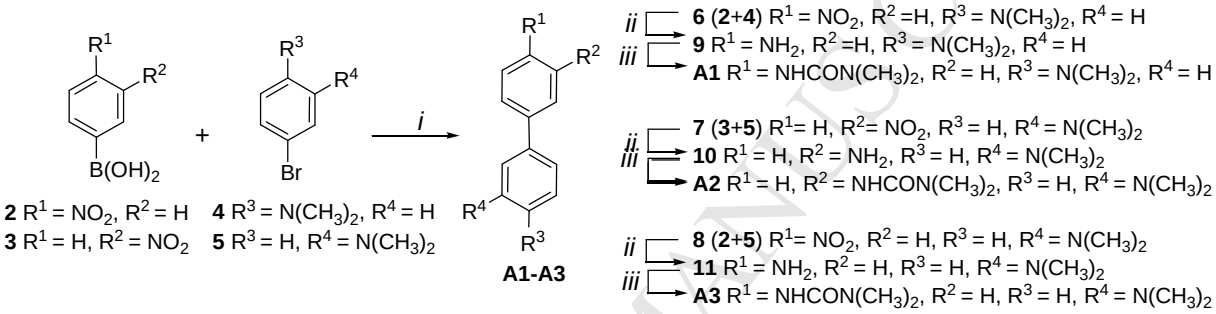

Scheme 1. Synthesis of series **A** : (*i*): Pd(dppf)Cl_2*DCM, CsF, dry DME, 80°C, overnight, **6** (40%), **7** (80%), **8** (85%); (*ii*): Pd/C 10%, H_2, DCM, R.T., overnight, quantitative yield; (*iii*): $ClCON(CH_3)_2$, Et_3N, dry DCM, 0°C-R.T., **A1** (46%), **A2** (46%), **A3** (36%).

The effect of the presence of only the *N*,*N*-dimethyl or carbamate or moiety as well as their position on the biaryl core (*meta* or *para*) was investigated by the series **B** and **C** (Figure 1 and Scheme 2 and 3). Analogues **B1** and **B2** bearing one *N*,*N*-dimethyl moiety at para and meta position were obtained from the commercially available 3- and 4-aminobiphenyl (**12** and **13**) using dimethylsulfate as methylation agent. Both the disubstituted and trisubstituted products were isolated. Since disubstituted, trisubstituted, and tetrasubstituted amines were obtained, **B1** and **B2** were obtained with low yield. Corresponding analogues **C1** and **C2** were obtained through the condensation of amines **12** and **13** with dimethylcarbamoyl chloride under basic conditions.

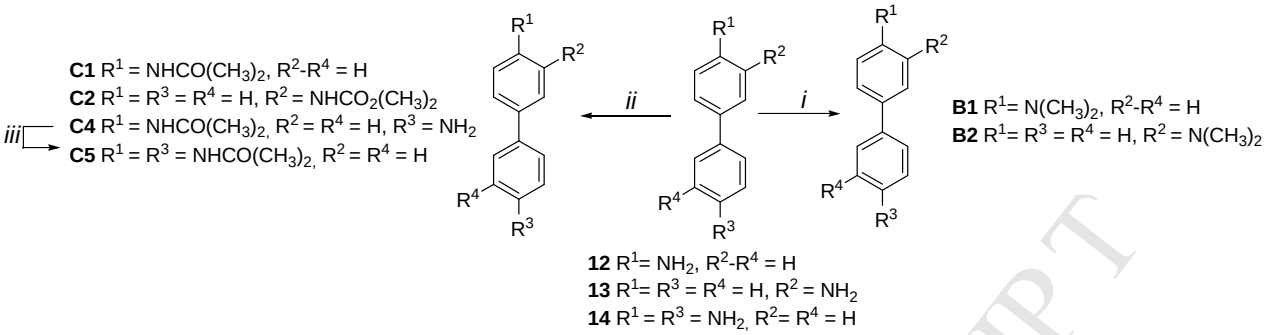

Scheme 2. Synthesis of series **B** and **C**: (*i*): Me_2SO_4, K_2CO_3, THF/H_2O, R.T., 24h, **B1** (11%), **B2** (14%); (*ii*): $ClCON(CH_3)_2$, Et_3N, dry DCM, 0°C-R.T., **C1** (47%), **C2** (37%), **C4** (70%); (*iii*): $ClCON(CH_3)_2$, piperidine, dry THF, 0°C-R.T., **C5** (5%).

Analogues bearing two *N*,*N*-dimethyl or carbamate moieties were further investigated. While 4,4'-Bis(dimethylamino)biphenyl (**B4**, Figure 2) was commercially available, the remaining analogues (**B3**, **C3**, **C5**) *N*,*N*-dimethyl or carbamate moieties were obtained as shown in scheme 2 and 3.

The reaction with benzidine (**14**) did not produce the disubstituted product **C5**, only the monosubstituted product **C4** was obtained (Scheme 2). As the first substitution occurred, the monosubstituted product **C4** precipitated due to its poor solubility. Furthermore, the second amine is not reactive enough to perform the nucleophile attack on the acyl chloride. To resolve this problem, compound **C4** was solubilized in THF and piperidine was used as base. Compound **C5** was obtained with a yield of 5%, demonstrating the poor reactivity of the aniline.

Analog **B3** (scheme 3) was synthesized starting from 3-(*N*,*N*-Dimethylamino)phenylboronic acid **15**, using a copper(I)-catalyzed homocoupling [19]**.** This reaction is useful for the synthesis of symmetric biaryl compound with mild reaction condition. Multiple side products were formed due to the degradation of the boronic acid. Therefore, **B3** was obtained only with a yield of 29%.

Analogue **C3** (scheme 3) was synthesized in a similar fashion to compounds **A1-A3**. 3,3'-biphenyldiamine (**18**) was obtained through copper(I)-catalyzed homocoupling [19] conditions of 3-Nitrophenylboronic acid (**16**) followed by a catalytic hydrogenation over Pd/C. Condensation of amine (**18**) with dimethylcarbamoyl chloride afford analog **C3**.

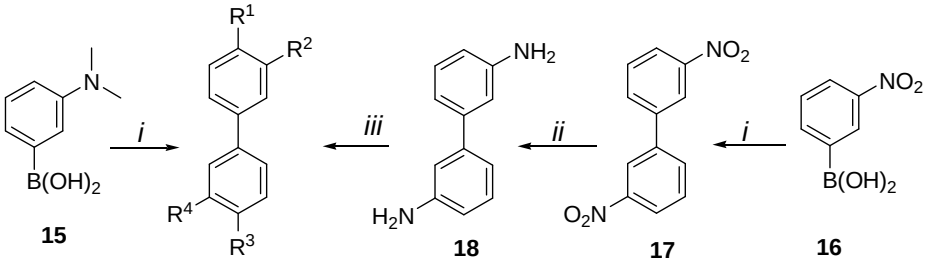

B3 $R^1 = R^3 = H$, $R^2 = R^4 = N(CH_3)_2$
C3 $R^1 = R^3 = H$, $R^2 = R^4 = NHCO(CH_3)_2$

Scheme 3. Synthesis of series **B** and **C** : (*i*): CuCl, MeOH, R.T., air, **B3** (29%), **17** (34%); (*ii*): Pd/C 10%, DCM, H_2, R.T., overnight, quantitative yield; (*iii*): $ClCON(CH_3)_2$, Et_3N, dry DCM, 0°C-R.T., **C3** (36%)

To investigate whether the biaryl central core of Atglistatin (**1**) is necessary for ATGL inhibition, analogues bearing only an aryl substituted with *N*,*N*-dimethyl or carbamate moieties were synthesized (**D1**-**D3**, scheme 4). Condensation of commercially available amines **19** and **20** with dimethylcarbamoyl chloride affords analogues **D1** and **D2**. **D2** and **D1** are the analogues of Atglistatin (**1**) and **A1,** respectively. Analogue **D3**, bearing two carbamate moieties in *para* position, was obtained from amine **21** through condensation with dimethylcarbamoyl chloride (scheme 4). A pre-treatment with base was required to obtain amine **21** form the corresponding hydrochloride salt.

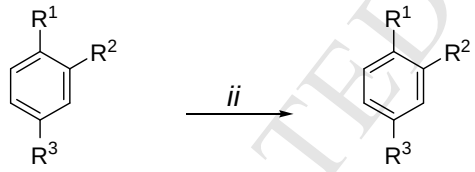

19 $R^1 = NH_2$, $R^2 = H$, $R^3 = N(CH_3)_2$
20 $R^1 = H$, $R^2 = NH_2$, $R^3 = N(CH_3)_2$
21 $R^1 = NH_2$, $R^2 = H$, $R^3 = NH_2$

D1 $R^1 = NHCON(CH_3)_2$, $R^2 = H$, $R^3 = N(CH_3)_2$
D2 $R^1 = H$, $R^2 = NHCON(CH_3)_2$, $R^3 = N(CH_3)_2$
D3 $R^1 = NHCON(CH_3)_2$, $R^2 = H$, $R^3 = NHCON(CH_3)_2$

Scheme 4. Synthesis of series **D**: (*i*): $ClCON(CH_3)_2$, Et_3N, dry DCM, 0°C-R.T., **D1** (81%), **D2** (67%), **D3** (42%).

Even after repeated attempts, we were not able to obtain the corresponding analogue with two carbamate moieties in *meta* position. Analogues **D4** and **D5** (Figure 2) bearing two *N*,*N*-dimethyl moieties at *para and meta* position were commercially available.

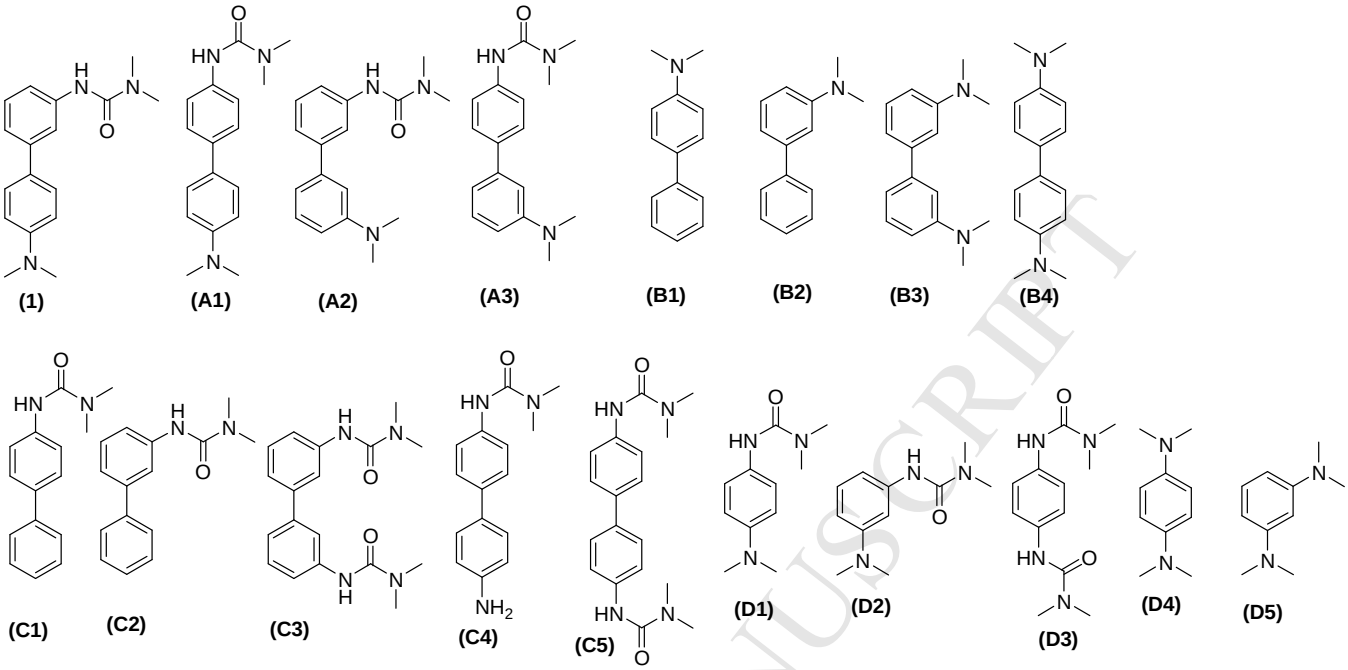

Figure 2. Structures of synthesized Atglistatin (**1**) closely related analogues.

2.2. ATGL inhibitory activity

The potential of our Atglistatin analogues to inhibit ATGL was examined indirectly by determining their effect on isoproterenol-stimulated lipolysis in 3T3-L1 adipocytes (Figure 3-5). Following incubation of adipocytes with the analogues for 1 h, concentrations of released non-esterified FA (NEFA) and glycerol, products of lipolysis, were measured in the media. The substitution of the central biaryl core seems to be crucial for inhibition of lipolysis and thus ATGL activity with Atglistatin (**1**). In fact, the analogue **A1** in which the carbamate group is in the *para* position was completely inactive (Figure 3). This change, which seems minor, causes a total inactivation of compound **A1** since levels of NEFA in the media from adipocytes incubated with **A1** were similar when compared to controls. The analogue **A2**, in which the *N,N*-dimethyl moiety is this time in the *meta* position, also appears to lose inhibitory effectiveness as compared to Atglistatin (**1**) (Figure 3). The interconversion of the two groups as shown with analogue **A3** compared to Atglistatin (**1**) causes also a complete inactivation. The total loss of activity with **A1**, **A2**, and **A3** clearly shows that the substitution pattern, position 3 and 4', is necessary for inhibition of ATGL with Atglistatin (**1**). More specifically, the carbamate moiety must be at position 3 and the *N,N*-dimethyl moiety at position 4'. Co-crystallization of Atglistatin (**1**) with ATGL would confirm the presence of favorable interactions with these two substituents.

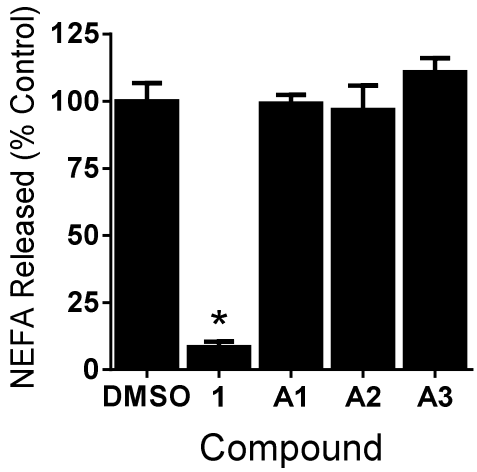

Figure 3. Effect of Series **A** compounds on NEFA release. 3T3-L1 adipocytes were incubated in DMEM containing 2% FA-free BSA in the presence of 2 µM isoproterenol for 1 hour plus the indicated compounds. NEFA content of incubation media was determined and normalized to cellular protein content. NEFA release is presented as % of control (incubated with DMSO), which was determined to be 111.83 nmol NEFA/hr · mg protein. Data are means ± SD. N=3, *$p < 0.05$.

To investigate the importance of the carbamate and the *N*,*N*-dimethyl moieties, series **B** and **C**, in which these groups are absent, were synthesized. As shown in Figure 4, the presence of the carbamate moiety was necessary for the inhibition of ATGL by Atglistatin (**1**). Analogues **B1** and **B2**, bearing only *N*,*N*-dimethyl at *para* or *meta* position lost any inhibitory activity compared to Atglistatin (1) (Figure 4a). Even the presence of two *N*,*N*-dimethyl moieties at *para* or *meta* positions as in analogues **B3** and **B4** resulted in a complete loss of ATGL inhibition.

The presence of only the carbamate moiety on the biaryl central core of Atglistatin (**1**) does not seem to be as beneficial for ATGL inhibition as demonstrated by the series **C** (Figure 4b). Only with the mono-substituted analogue **C2**, in which the carbamate group was in the *meta* position as in Atglistatin (**1**) (see Figure 2), a slight inhibition was observed. Otherwise the di-substituted analogues with carbamate moiety at *para* or *meta* position (**C3** and **C5**) are completely inactive. Interestingly, the intermediate **C4**, which served for the preparation of **C5**, in which there is a free amine at the *para* position, results in a slight, but significant activation of lipolysis, suggesting a moderate increase in ATGL activity.

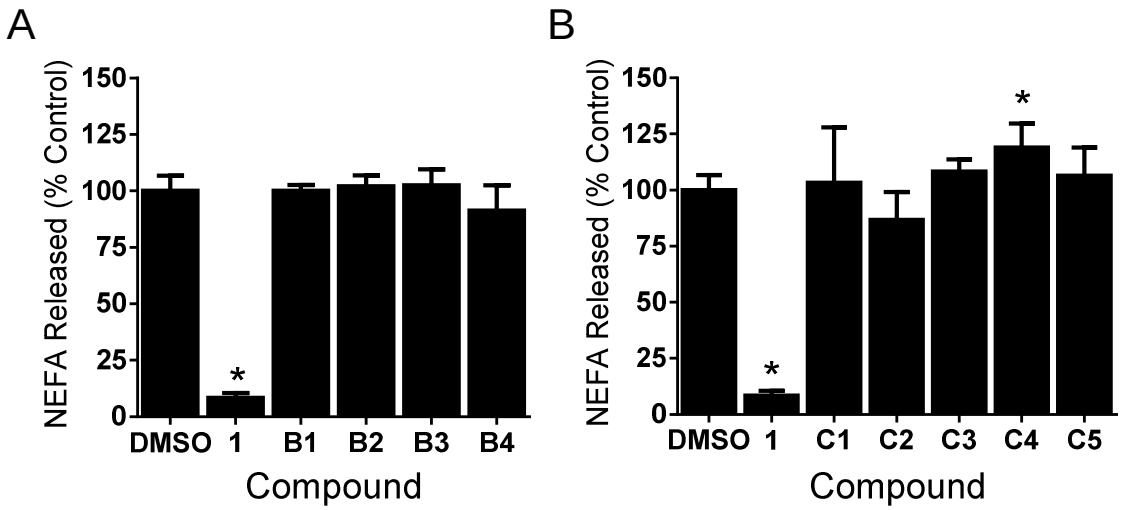

Figure 4. Effect of Series **B** and **C** compounds on NEFA release. 3T3-L1 adipocytes were incubated in DMEM containing 2% FA-free BSA in the presence of 2 µM isoproterenol for 1 hour plus the indicated compounds. NEFA content of incubation media was determined and normalized to cellular protein content. NEFA release is presented as % of control (incubated with DMSO), which was determined to be 111.83 nmol NEFA/hr · mg protein. Data are means ± SD. N=3, *$p < 0.05$.

The presence of a central aryl core instead of a biaryl does not seem to be beneficial for ATGL inhibition as shown by the series **D** (Figure 5). Analogues bearing the carbamate and/or *N*,*N*-dimethyl moiety have no effect on lipolysis. Even analogue **D2**, bearing the same groups as Atglistatin (1) at *meta* and *para* positions, has no effect. Analogues with only two carbamates or *N*,*N*-dimethyl moieties (**D3**, **D4**, **D5**) were not active compared to Atglistatin (**1**). A decrease of the lipophilic character and the loss of favorable interactions with the enzyme may explain this total loss of activity.

Free glycerol quantification gave the same results as the quantification of NEFA; none of the synthesized analogues showed significant changes in free glycerol release as compared to control (data not shown). Only the mono-substituted analogue **C2**, in which the carbamate group was in the *meta* position as in Atglistatin (**1**) (see Figure 2) showed a slight reduction in the free glycerol concentration in the media.

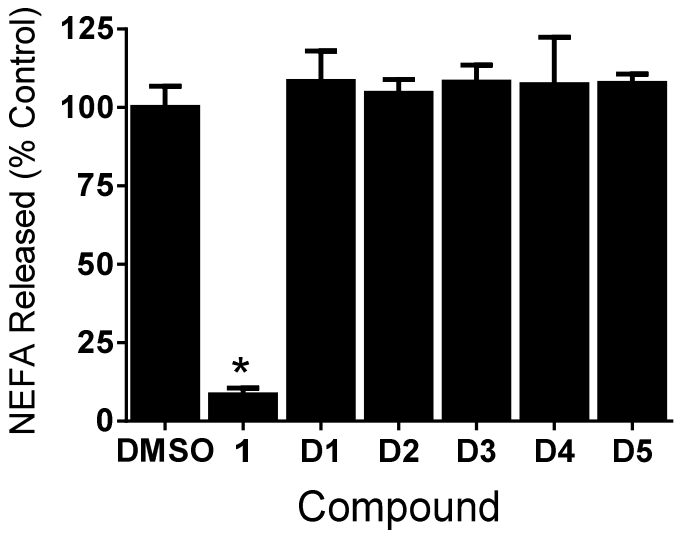

Figure 5. Effect of Series **D** compounds on NEFA release. 3T3-L1 adipocytes were incubated in DMEM containing 2% FA-free BSA in the presence of 2 µM isoproterenol for 1 hour plus the indicated compounds. NEFA content of incubation media was determined and normalized to cellular protein content. NEFA release is presented as % of control (incubated with DMSO), which was determined to be 111.83 nmol NEFA/hr · mg protein. Data are means ± SD. N=3, *$p < 0.05$.

To understand the large difference in activity between Atglistatin (**1**) and its closest analogues **A1**-**A3**, minimal energy as well as dipole moment of these structures were calculated. Differences in structure, total minimal energy and dipole moment are apparent from Table 1 and Figure 6. Although compound **A2** has comparable total energy and also has a planar structure like Atglistatin (**1**), **A2** as well as **A1** and **A3** have higher dipole moments than Atglistatin (**1**), possibly explaining their lower inhibitory potential. It has been shown that dipole moment can play a key role in drug-receptor interactions [20].

Table 1. Minimal energy and dipole moment of Atglistatin (**1**) and **A1-A3**

Compounds	Total energy (a.u.)	Dipole moment (Debye)
Atglistatin (**1**)	-899.7058355	1.6485
(**A1**)	-899.6949831	4.476
(**A2**)	-899.7051396	4.3191
(**A3**)	-899.6949241	4.1744

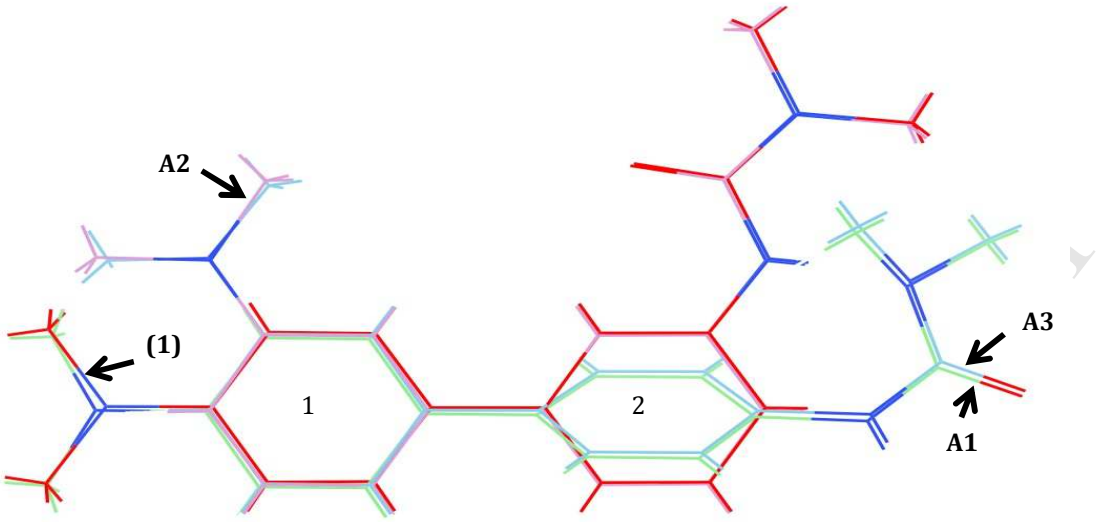

Figure 6. Molecules are aligned to have overlapping ring 1 in all for cases. Ring 2 is in the same plane as ring 1 for Atglistatin (**1**) and (**A2**) and is perpendicular to the plane of the ring 1 for (**A3**) and (**A13**).

Conclusions

In summary, the present study shows clearly that inhibition of ATGL by Atglistatin (**1**) is due to the presence of the carbamate and *N*,*N*-dimethyl moieties on the biaryl central core at the *meta* and *para* position, respectively. Moving the carbamate or the *N*,*N*-dimethyl in the *para* or *meta* position results in a total loss of ATGL inhibition as compared to Atglistatin (**1**). As the binding area of Atglistatin (**1**) on ATGL was rather sensitive to any modifications made on the structure of Atglistatin (**1**), these results may lead to the identification of the pharmacophore groups on Atglistatin, which brings new insights on the chemical interactions between ATGL and potential Atglistatin (**1**)-based inhibitors. Due the lack of a crystal structure of ATGL, the present structure activity relationship study should assist the development of future ATGL inhibitors.

4. Experimental section

4.1. Chemistry

All chemicals used were purchased from Aldrich (CA). Purification of compounds was carried out by flash chromatography (CombiFlash®, Separation System SG 100C, ISCO) or by silica gel circular chromatography (chromatotron®, model 7924, Harrison Research). TLC was run on silica gel coated aluminium sheets (SiliaPlate TLC, Silicycle®) with detection by UV light (254 nm, UVS-11, Mineralight® shortwave UV lamp). Melting points were obtained using a

MELTEMP (model 1001D) melting point apparatus. FTIR spectra were recorded on a Nicolet Impact 400 spectrometer. NMR spectra were recorded on a Bruker Avance III 400 MHz spectrometer.

***General Procedure I**: Suzuki-Miyaura coupling*

Boronic acid, aryl halide, Pd(dppf)Cl_2*DCM, CsF, and dry dimethoxyethane (DME) were introduced in a 100 ml shlenk tube. The reaction mixture was flushed three times by vacuum/argon and stirred at 80 °C overnight. The reaction mixture was filtered through celite and rinsed with EtOAc. The solvent was removed under vacuum and the residue was purified by flash column chromatography (EtOAc-hexane).

***General procedure II**: catalytic hydrogenation of nitro analogues*

Pd/C (10%) was added to a solution of the appropriate nitro compound in CH_2Cl_2. The reaction mixture was stirred under hydrogen atmosphere until completion (verified by TLC). The reaction mixture was filtered through celite and rinsed with EtOAc. The solvent was removed under vacuum and the amine structure was confirmed by NMR analysis. The product was used for the next experiment without any further purification.

***General Procedure III**: Carbamate from aniline and dimethylcarbamoyl chloride*

Triethylamine (1 eq. per amine) was added to a stirred solution of the appropriate amine in dry dichloromethane. The reaction vessel was flushed with argon and cooled with an ice bath. Dimethylcarbamoyl chloride (1.3 eq. per amine) was added dropwise and the reaction vessel was flushed again with argon. The mixture was left to react at room temperature. During the reaction, additional portions of dimethylcarbamoyl chloride may be added. At the end of the reaction (verified by TLC), the solution was hydrolyzed with water. The organic layer was separated and the aqueous layer was extracted twice with EtOAc. The combined organic phase was washed twice with brine, dried ($MgSO_4$), and concentrated under vacuum. The resulting product was purified by flash chromatography.

4-Nitro-4'-(dimethylamino)-biphenyl (**6**)

Following general procedure I with 4-nitrophenylboronic acid (1.28 g, 7.65 mmol), 4-bromo-*N*,*N*-dimethylaniline (1.469 g, 7.34 mmol), Pd(dppf)Cl_2*DCM (345.02 mg, 0.42 mmol), CsF (2.412 g, 15.88 mmol), and DME (10 mL), a reddish solid was obtained after flash chromatography purification (EtOAc-hexane 0→ 25%). Yield = 370 mg (40%); R_f = 0.65

(EtOAc-hexane 1:9); m.p. = 236-239 °C; ^{1}H NMR (400 MHz, $CDCl_3$, 25°C), δ (ppm): 8.27-8.24 (m, 2H, H_{ar}), 7.71-7.69 (m, 2H, H_{ar}), 7.59-7.57 (m, 2H, H_{ar}), 6.83-6.81 (m, 2H, H_{ar}), 3.06 (s, 6H, $ArN(CH_3)_2$); ^{13}C NMR (100 MHz, $CDCl_3$, 25°C) δ (ppm): 150.96, 147.63, 145.80, 128.12, 126.08, 125.81, 124.19, 112.50, 40.29.

4-Amino-4'-(dimethylamino)-biphenyl (**9**)

Following general procedure II with **6** (185 mg, 0.76 mmol), CH_2Cl_2 (5 mL), and Pd/C (10%, 30 mg), a brownish liquid was obtained. Quantitative yield; ^{1}H NMR (400 MHz, $CDCl_3$, 25°C), δ (ppm) 7.48-7.46 (m, 2H, H_{ar}), 7.41-7.39 (m, 2H, H_{ar}), 6.84-6.82 (m, 2H, H_{ar}), 6.78-6.75 (m, 2H, H_{ar}), 3.00 (s, 6H, $ArN(CH_3)_2$); ^{13}C NMR (100 MHz, $CDCl_3$, 25°C) δ (ppm): 149.43, 144.77, 131.95, 129.73, 127.23, 127.04, 115.52, 113.03, 40.77.

4-(3,3-dimethylureido)-4'-(dimethylamino)-biphenyl (**A1**)

Following general procedure III with **9** (178 mg, 0.82 mmol), Et_3N (120 µL, 0.86 mmol), CH_2Cl_2 (5 mL), and 150 µL of dimethylcarbamoyl chloride (an additional 150 µl was added during the reaction, to a total of 3.26 mmol), a beige solid was obtained after purification by flash chromatography (EtOAc-hexane 0→ 40%). Yield = 105.6 mg (46%); R_f = 0.20 (EtOAc-hexane 1:1); m.p. = 228-230°C; ^{1}H NMR (400 MHz, $CDCl_3$, 25°C), δ (ppm): 7.51-7.42 (m, 6H, H_{ar}), 6.83-6.81 (m, 2H, H_{ar}), 6.36 (s, 1H, ArNHCO-), 3.06 (s, 6H, $-CON(CH_3)_2$), 3.01 (s, 6H, $ArN(CH_3)_2$); ^{13}C NMR (100 MHz, $CDCl_3$, 25°C), δ (ppm): 155.77, 149.74, 137.38, 136.01, 129.01, 127.33, 126.59, 120.19, 112.89, 40.66, 36.49; HRMS *m/s* calc. for $C_{17}H_{21}N_3O$ + (H^+): 284.1757; found: 284.1759.

3-*Nitro-3'-(dimethylamino)-biphenyl* (**7**)

Following general procedure I with 3-nitrophenylboronic acid (1.25 g, 7.50 mmol), 3-bromo-*N*,*N*-dimethylaniline (1.07 ml, 7.50 mmol), $Pd(dppf)Cl_2$*DCM (372.36 mg 0.46 mmol), CsF (2.87 g, 18.89 mmol), and DME (10 mL), an orange solide was obtained after purification by flash chromatography (EtOAc-hexane 0→ 20%). Yield = 1.44 g (80 %); R_f = 0.65 (EtOAc-hexane 1:9); m.p. = 55-58 °C; ^{1}H NMR (400 MHz, $CDCl_3$, 25°C), δ (ppm): 8.48-8.47 (m, 1H, H_{ar}), 8.22-8.20 (m, 1H, H_{ar}), 7.95-7.92 (m, 1H, H_{ar}), 7.63-7.59 (m, 1H, H_{ar}), 7.39-7.35 (m, 1H, H_{ar}), 6.98-6.96 (m, 1H, H_{ar}), 6.93-6.92 (m, 1H, H_{ar}), 6.84-6.81 (m,1H, H_{ar}), 3.06 (s, 6H, $ArN(CH_3)_2$), ^{13}C NMR (100 MHz, $CDCl_3$, 25°C) δ (ppm): 151.09, 148.64, 143.96, 139.73,

133.28, 129.83, 129.49, 122.10, 121.86, 115.46, 112.57, 111.04, 40.63; HRMS *m/s* calc. for $C_{14}H_{14}N_2O_2$ + (H^+): 243.1128; found: 243.1135.

3-Amino-3'-(dimethylamino)-biphenyl (**10**)

Following general procedure II with **7** (263 mg, 1.08 mmol), CH_2Cl_2 (5 mL), and Pd/C (10%, 15 mg), a brownish liquid was obtained. Quantitative yield; ^{1}H NMR (400 MHz, $CDCl_3$, 25°C), δ (ppm): 7.34-7.30 (m, 1H, H_{ar}), 7.26-7.22 (m, 1H, H_{ar}), 7.04-7.02 (m, 1H, H_{ar}), 6.96-6.94 (m, 3H, H_{ar}), 6.78-6.75 (m, 1H, H_{ar}), 6.71-6.69 (m, 1H, H_{ar}), 3.77 (s, 2H, $ArNH_2$), 3.03 (s, 6H, $ArN(CH_3)_2$); ^{13}C NMR (100 MHz, $CDCl_3$, 25°C), δ (ppm): 150.85, 146.58, 143.51, 142.46, 129.51, 129.29, 117.93, 115.89, 114.16, 113.98, 111.69, 111.64.

3-(3,3-dimethylureido)-3'-(dimethylamino)-biphenyl (**A2**)

Following general procedure III with **10** (211 mg, 0.97 mmol), Et_3N (150 µL, 1.08 mmol), CH_2Cl_2 (5 mL), and 150 µL of dimethylcarbamoyl chloride (an additional portion of 150 µL was added during the reaction, to a total of 3.26 mmol), a white solid was obtained after purification by flash chromatography (EtOAc-hexane 0→ 40%). Yield = 125 mg (46%); R_f = 0.20 (EtOAc-hexane 1:1); m.p. = 180-181 °C; ^{1}H NMR (400 MHz, $CDCl_3$, 25°C), δ (ppm): 7.55 (s, 1H, H_{ar}), 7.47-7.45 (m, 1H, H_{ar}), 7.38-7.28 (m, 3H, H_{ar}), 6.98-6.94 (m, 2H, H_{ar}), 6.77-6.74 (m, 1H, H_{ar}), 6.42 (s, 1H, ArNHCO-), 3.06 (s, 3H, -$CON(CH_3)_2$), 3.02 (s, 3H, $ArN(CH_3)_2$); ^{13}C NMR (100 MHz, $CDCl_3$, 25°C), δ (ppm): 155.75, 150;91, 142.99, 142.01, 139.41, 129.31, 129.10, 122.07, 118.72, 115.95, 111.75, 111.60, 40.74, 36.50; HRMS *m/s* calc. for $C_{17}H_{21}N_3O$ + (H^+): 284.1757; found: 284.177.

4-*Nitro-3'-(dimethylamino)-biphenyl* (**8**)

Following general procedure I with 4-nitrophenylboronic acid (1.28 g, 7.67 mmol), 3-bromo-*N*,*N*-dimethylaniline (1.07 ml, 7.50 mmol), Pd(dppf)Cl_2*DCM (401.39 mg, 0.49mmol), CsF (2.47 g, 16.26 mmol), and DME (10 mL) a yellow solid was obtained after column purification (EtOAc-hexane 0→ 10%). Yield = 1.58 g (85%); R_f = 0.38 (EtOAc-hexane 1:9); m.p. = 138-140 °C; ^{1}H NMR (400 MHz, $CDCl_3$, 25°C), δ (ppm): 8.81-8.29 (m, 2H, H_{ar}), 7.77-7.75 (m, 2H, H_{ar}), 7.40-7.36 (m, 1H, H_{ar}), 6.98-6.96 (m, 1H, H_{ar}), 6.92 (s, 1H, H_{ar}), 6.85-6.82 (m, 1H, H_{ar}), 3.06 (s, 6H, $ArN(CH_3)_2$); ^{13}C NMR (100 MHz, $CDCl_3$, 25°C), δ (ppm): 151.02, 148.78, 146.96, 139.81, 129.81, 127.93, 123.95, 115.67, 112.94, 111.19, 40.59; HRMS *m/s* calc. for $C_{14}H_{14}N_2O_2$ + (H^+): 243.1128; found: 243.112.

4-Amino-3'-(dimethylamino)-biphenyl (**11**)

Following general procedure II with **8** (249 mg, 1.03 mmol), CH_2Cl_2 (8 mL), and Pd/C (10%, 15 mg), a brown liquid was obtained. Quantitative yield; ^{1}H NMR (400 MHz, $CDCl_3$, 25°C), δ (ppm): 7.46-7.43 (m, 2H, H_{ar}), 7.33-7.28 (m, 1H, H_{ar}), 6.96-6.95 (m, 2H, H_{ar}), 6.79-6.75 (m, 3H, H_{ar}), 3.03 (s, 6H, $ArN(CH_3)_2$); ^{13}C NMR (100 MHz, $CDCl_3$, 25°C), δ (ppm): 150.65, 145.75, 142.27, 132.49, 129.36, 128.18, 115.94, 115.28, 111.35, 111.21, 41.03.

4-(3,3-dimethylureido)-3'-(dimethylamino)-biphenyl (**A3**)

Following general procedure III with **11** (225 mg, 1.03 mmol), Et_3N (150 µL, 1.08 mmol), CH_2Cl_2 (5mL), and 200 µL of dimethylcarbamoyl chloride (multiple additions during the reaction to a total of 1.30 ml (14.11 mmol)), a white solid was obtained after purification by flash chromatography (EtOAc-hexane 0→ 50%). Yield = 106.5 mg (36%); R_f = 0.41 (EtOAc-hexane 1:1); m.p. = 180-181 °C; ^{1}H NMR (400 MHz, $CDCl_3$, 25°C), δ (ppm): 7.56-7.54 (m, 2H, H_{ar}), 7.47-7.45 (m, 2H, H_{ar}), 7.33-7.29 (m, 1H, H_{ar}), 6.96-6.93 (m, 2H, H_{ar}), 6.75-6.73 (m, 1H, H_{ar}), 6.39 (s, 1H, ArNHCO-), 3.07 (s, 6H, $-CON(CH_3)_2$), 3.02 (s, 6H, $ArN(CH_3)_2$); ^{13}C NMR (100 MHz, $CDCl_3$, 25°C), δ (ppm): 155.69, 150.98, 141.76, 138.39, 136.83, 129.36, 127.65, 119.95, 115.54, 111.36, 111.25, 40.75, 36.50; HRMS *m/s* calc. for $C_{17}H_{21}N_3O$ + (H^+): 284.1757; found: 284.177.

4-(dimethylamino)-biphenyl (**B1**)

Dimethyl sulfate (370 µL, 3.96 mmol) was added to a vigorously stirred solution of 4-aminobiphenyl (500 mg, 2.98 mmol) in THF (6 mL). Afterward, a solution of K_2CO_3 (540 mg, 3.96 mmol) in water (5 mL) was added and the reaction was left to react at room temperature for 24h. The solution was suspended in EtOAc (30 mL) and the phases were separated. The aqueous phase was extracted with EtOAc (3 x 30 mL). The combined organic phase were washed with brine (3 x 15 mL), dried ($MgSO_4$) and concentrated under vacuum. A yellow solid was obtained after purification by flash chromatography (EtOAc-hexane 0→ 3%). Yield = 66 mg (11%); R_f = 0.63 (EtOAc-hexane 1:9); m.p. = 118-120°C; ^{1}H NMR (400 MHz, $CDCl_3$, 25°C), δ (ppm): 7.61-7.59 (m, 2H, H_{ar}), 7.56-7.54 (m, 2H, H_{ar}), 7.45-7.41 (m, 2H, H_{ar}), 7.31-7.27 (m, 1H, H_{ar}), 6.86-6.84 (m, 2H, H_{ar}), 3.03 (s, 6H, $-N(CH_3)_2$); ^{13}C NMR (100 MHz, $CDCl_3$, 25°C), δ (ppm):150.00, 141.25, 129.29, 128.65, 127.72, 126.31, 126.00, 112.80, 40.61; HRMS *m/s* calc. for $C_{14}H_{15}N$ + (H^+): 198.1277; found: 198.1279.

3-(Dimethylamino)-biphenyl (**B2**)

Dimethyl sulfate (200 µL, 1.95 mmol) was added to a vigorously stirred solution of 3-aminobiphenyl (250 mg, 1.49 mmol) in THF (6 mL). Afterward, a solution of K_2CO_3 (270 mg, 1.95 mmol) in water (5 mL) was added and the reaction was left to react at room temperature for 24h. The solution was suspended in EtOAc (30 mL) and the phases were separated. The aqueous phase was extracted with EtOAc (3 x 30 mL). The combined organic phase was washed with brine (3 x 15 mL), dried ($MgSO_4$) and concentrated under vacuum. A yellow liquid was obtained after flash chromatography (EtOAc-hexane 0→ 14%). Yield = 40 mg (14%); R_f = 0.63 (EtOAc-hexane 1:9); ^{1}H NMR (400 MHz, $CDCl_3$, 25°C), δ (ppm): 7.65-7.63 (m, 2H, H_{ar}), 7.49-7.45 (m, 2H, H_{ar}), 7.39-7.28 (m, 2H, H_{ar}), 7.00-6.98 (m, 1H, H_{ar}), 6.97 (s, 1H, H_{ar}), 6.80-6.78 (m, 1H, H_{ar}), 3.05 (s, 6H, -N(CH_3)$_2$); ^{13}C NMR (100 MHz, $CDCl_3$, 25°C), δ (ppm): 150.97, 142.30, 129.42, 128.60, 127.36, 127.09, 115.87, 111.66, 111.61, 40.74; HRMS *m/s* calc. for $C_{14}H_{15}N$ + (H^+): 198.1277, found: 198.1285.

4-(3,3-dimethylureido)-biphenyl (**C1**)

Following general procedure III with 4-aminobiphenyl (505 mg, 2.98 mmol), Et_3N (420 µL, 2.98 mmol), CH_2Cl_2 (8 mL), and 420µL of dimethylcarbamoyl chloride (an additional 1 ml was added during the reaction, to a total of 15.42 mmol), a white solid was obtained after purification by flash chromatography (EtOAc-hexane 0→ 30%). Yield = 336 mg (47%); m.p. = 176-178°C; R_f = 0.19 (EtOAc-hexane 1:1). ^{1}H NMR (400 MHz, $CDCl_3$, 25°C), δ (ppm): 7.61-7.54 (m, 4H, H_{ar}), 7.50-7.42 (m, 4H, H_{ar}), 7.35-7.31 (m, 1H, H_{ar}), 6.44 (s, 1H, -NHCO-), 3.07 (s, 6H, -CON(CH_3)$_2$); ^{13}C NMR (100 MHz, $CDCl_3$, 25°C), δ (ppm): 155.65, 140.75, 138.58, 135.77, 128.72, 127.49, 126.84, 126.76, 120.05, 36.50; HRMS *m/s* calc. for $C_{15}H_{16}N_2O$ + (H^+): 241.1335, found: 241.1347.

3-(3,3-dimethylureido)-biphenyl (**C2**)

Following general procedure III with 3-aminobiphenyl (250 mg, 1.49 mmol), Et_3N (210 µL, 1.49 mmol), CH_2Cl_2 (8 mL), and 201 µL of dimethylcarbamoyl chloride (an additional 500 µL was added during the reaction, to a total of 9.00 mmol), a white solid after purification by flash chromatography (EtOAc-hexane 0→ 20%). Yield = 132 mg, 37%; m.p. 152-155°C; R_F 0.25 (EtOAc-hexane 1:1); ^{1}H NMR (400 MHz, $CDCl_3$, 25°C), δ (ppm): 7.68 (s, 1H, H_{ar}), 7.63-7.61 (m, 2H, H_{ar}), 7.46-7.42 (m, 2H, H_{ar}), 7.40-7.28 (m, 4H, H_{ar}), 6.42 (s, 1H, -NHCO-), 3.07 (s, 6H, -CON(CH_3)$_2$); ^{13}C NMR (100 MHz, $CDCl_3$, 25°C), δ (ppm): 155.69, 141.98, 140.97, 139.58,

129.22, 128.65, 127.32, 127.21, 121.80, 118.65, 118,62, 36.49; HRMS *m/s* calc. for $C_{15}H_{16}N_2O$ + (H^+): 241.1335; found: 241.134.

4-Amino-4'-(3,3-dimethylureido)-biphenyl (**C4**)

Following general procedure III with benzidine (514 mg, 2.79 mmol), Et_3N (780 µL, 10.59 mmol), CH_2Cl_2 (8 mL), and 1.02 ml of dimethylcarbamoyl chloride (an additional 1 ml was added during the reaction, to a total of 16.11 mmol), a yellow solid was obtained after purification by flash chromatography (EtOAc-hexane 0→ 100%). There was only a mono-substitution because the product precipitated during the reaction. Yield = 500 mg (70%); m.p. >215°C; R_f = 0.56 (MeOH-CH_2Cl_2 1:20); ^{1}H NMR (400 MHz, $CDCl_3$, 25°C), δ (ppm): 7.49-7.39 (m, 6H, H_{ar}), 6.77-6.75 (m, 2H, H_{ar}), 6.35 (s, 1H, ArNHCO-), 3.75 (s, 2H, $ArNH_2$), 3.06 (s, 6H, $ArN(CH_3)_2$); ^{13}C NMR (100 MHz, $CDCl_3$, 25°C), δ (ppm): 155.73, 145.49, 137.59, 135.94, 131.23, 127.63, 126.71, 120.14, 115.41, 36.49; HRMS *m/s* calc. for $C_{15}H_{17}N_3O$ + (H^+): 256.1444; found: 256.1451.

4,4'-Bis-(3,3-dimethylureido)-biphenyl (**C5**)

Piperidine (563 µL, 5.96 mmol) was added to a vigorously stirred solution of **C4** (500 mg, 2.71 mmol) in dry THF (5 mL), The reaction vessel was thoroughly flushed with argon and cooled to 0°C with an ice bath. Dimethylcarbamoyl chloride (502 µL, 6.78 mmol) was added dropwise to the reaction an ice bath. The mixture was left to react at room temperature. At the end of the reaction (verified by TLC), the solution is hydrolysed with water (50 mL) and the phases were separated, the aqueous phase was extract with EtOAc (3 x 30 mL). The combined organic phase was washed with brine (3 x 15 mL), dried ($MgSO_4$), and concentrated. A brown-red solid was obtained after purification by chromatography on silica gel coated glass (2 X MeOH/CH_2Cl_2, 5%). Yield = 30 mg (5%); m.p. >350°C; R_f = 0.50 (MeOH/CH_2Cl_2 1:20); ^{1}H NMR (400 MHz, DMSO-d6, 25°C), δ (ppm): 8.35 (s, 2H, -NHCO-), 7.55-7.53 (m, 4H, H_{ar}), 7.51-7.49 (m, 4H, H_{ar}), 2.94 (s, 12H, $-CON(CH_3)_2$); ^{13}C NMR (100 MHz, DMSO-d6, 25°C), δ (ppm): 156.18, 140.09, 133.62, 126.25, 120.38, 36.74; HRMS *m/s* calc. for $C_{18}H_{22}N_4O_2$ + (H^+): 327.1816; found: 327.1817.

3,3'-Dinitrobiphenyl (**17**)

A solution of 3-nitrophenylboronic acid (1.45 g, 8.69 mmol) and CuCl (56.40 mg, an additionnal 40 mg was added during the reaction, to a total of 0.97 mmol) in methanol (20 mL) was stirred at 25 °C until reaction completion (TLC control). The reaction mixture was filtered through celite

and washed with EtOAc (30 mL). The combined filtrate was concentrated in vaccum and the residue was purified by flash chromatography (EtOAc-hexane 0→ 20%). A yellow solid was obtained. Yield 365.8 mg (34%); R_f = 0.56 (EtOAc-hexane 1:3); m.p. = 207-208 °C; ^{1}H NMR (400 MHz, $CDCl_3$, 25°C), δ (ppm): 8.53 (s, 2H, H_{ar}), 8.34-8.32 (m, 2H, H_{ar}), 8.01-7.99 (m, 2H, H_{ar}), 7.75-7.71 (m, 2H, H_{ar}); ^{13}C NMR (100 MHz, $CDCl_3$, 25°C), δ (ppm): 148.91, 140.35, 133.06, 130.31, 123.31, 122.12.

3,3'-Diaminobiphenyl (**18**)

Following general procedure II with **17** (235 mg, 0.96 mmol), CH_2Cl_2 (8 mL), and Pd/C (10%, 30 mg), a yellow oil was obtained. Quantitative yield; ^{1}H NMR (400 MHz, $CDCl_3$, 25°C), δ (ppm): 7.25-7.21 (m, 2H, H_{ar}), 7.00-6.98 (m, 2H, H_{ar}), 6.91-6.90 (m, 2H, H_{ar}), 6.70-6.68 (m, 2H, H_{ar}), 3.74 (s, 4H, $ArNH_2$); ^{13}C NMR (100 MHz, $CDCl_3$, 25°C), δ (ppm): 146.60, 142.64, 129.55, 117.68, 114.09, 113.92.

3,3'-Bis-(dimethylamino)-biphenyl (**B3**)

A solution of 3-(*N*,*N*-dimethylamino)phenylboronic acid (192 mg, 1.21 mmol) and CuCl (23.76 mg, 0.24 mmol) in methanol (10 mL) was stirred at 25 °C until reaction completion (verified by TLC). The reaction mixture was filtered through celite and washed with EtOAc (40 mL). The combined filtrate was concentrated in vacuum and the residue was purified by circular chromatography (EtOAc-hexane 0→ 10%). A brownish oil was obtained. Yield = 40.84 mg (29%); R_f = 0.88 (EtOAc-hexane 1:1); ^{1}H NMR (400 MHz, $CDCl_3$, 25°C), δ (ppm): 7.37-7.33 (m, 2H, H_{ar}), 7.01-6.99 (m, 4H, H_{ar}), 6.80-6.78 (m, 2H, H_{ar}), 3.04 (s, 12H, $2ArN(CH_3)_2$); ^{13}C NMR (100 MHz, $CDCl_3$, 25°C), δ (ppm): 150.89, 143.40, 129.25, 116.16, 111.98, 111.58, 40.79; HRMS *m/s* calc. for $C_{16}H_{20}N_2 + (H^+)$: 241.1699; found: 241.1698.

3,3'-Bis-(3,3-dimethylureido)-biphenyl (**C3**)

Following general procedure III with **18** (195 mg, 1.06 mmol), Et_3N (300 µL, 2.15 mmol), CH_2Cl_2 (5 mL), and 500 µL of dimethylcarbamoyl chloride (multiple additions during the reaction to a total of 1.40 ml (15.21 mmol)), a white solid was obtained after purification by flash chromatography (EtOAc-hexane 0→ 90%). Yield = 124.4 mg (36%) ; R_f = 0.32 (100% EtOAc); m.p. >250 °C; ^{1}H NMR (400 MHz, $CDCl_3$, 25°C), δ (ppm): 7.62 (s, 2H, H_{ar}), 7.43-7.41 (m, 2H, H_{ar}), 7.36-7.32 (m, 2H, H_{ar}), 7.28-7.27 (m, 2H, H_{ar}), 6.48 (s, 2H, ArNHCO-), 3.07 (s, 12H, -$CON(CH_3)_2$); ^{13}C NMR (100 MHz, $CDCl_3$, 25°C), δ (ppm):155.78, 141.66, 139.52, 129.15,

121.87, 118,82, 118.58, 36.51; HRMS *m/s* calc. for $C_{18}H_{22}N_4O_2$ + (H^+): 327.1816; found: 327.1829.

1-(3,3-Dimethylureido)-4-(dimethylamino)benzene (**D1**)

Following general procedure III with 500 mg of *p*-(dimethylamino)benzamine (3.67 mmol), Et_3N (1.51 mL, 20.57 mmol), CH_2Cl_2 (8 mL), and dimethylcarbamoyl chloride (1.340 mL, 10.65 mmol), a white solid was obtained after flash chromatography (EtOAc-hexane 0→ 60%). Yield = 618.9 mg (81%); R_f = 0.28 (EtOAc 100%); m.p. = 170°C; ^{1}H NMR (400 MHz, $CDCl_3$, 25°C), δ (ppm): 7.25-7.21 (m, 2H, H_{ar}), 6.73-6.71 (m, 2H, H_{ar}), 6.16 (s, 1H, -CHCO-), 3.02 (s, 6H, -$CON(CH_3)_2$), 2.92 (s, 6H, -$N(CH_3)_2$); ^{13}C NMR (100 MHz, $CDCl_3$, 25°C), δ (ppm): 156.48, 147.58, 129.16, 122.48, 113.47, 41.19, 36.44; HRMS *m/s* calc. for $C_{11}H_{17}N_3O$ + (H^+): 208.1444; found: 208.1455.

1-(3,3-Dimethylureido)-3-(dimethylamino)benzene (**D2**)

N,*N*-Dimethyl-1,3-phenylenediamine dihydrochloride (700 mg, 3.34 mmol) was treated with K_2CO_3 (4 g, 28.9 mmol) in water (5 mL). After 2 hour, the *m*-(dimethylamino)benzenamine was extracted from the aqueous phase with dichloromethane (3 X 20 mL). The organic phase was dried ($MgSO_4$) and concentrated under vacuum. *m*-(Dimethylamino)benzenamine was obtained with a yield of 45% (440 mg). Following general procedure III with 440 mg *m*-(dimethylamino)benzenamine (3.23 mmol), 470 µL of Et_3N (3.34 mmol) and 460 µL of dimethylcarbamoyl chloride (5.01 mmol), compound **D2** was obtained as a beige solid after flash chromatography (EtOAc-hexane 0→ 40%). Yield = 448.2 mg (67%); R_f = 0.13 (EtOAc-hexane 1:1); m.p. = 124-126°C; ^{1}H NMR (400 MHz, $CDCl_3$, 25°C), δ (ppm): 7.16-7.12 (m, 1H, H_{ar}), 7.05-7.03 (m, 1H, H_{ar}), 6.62-6.60 (m, 1H, H_{ar}), 6.46-6.43 (m, 1H, H_{ar}), 6.30 (s, 1H, -NHCO-), 3.04, (s, 6H, -$CON(CH_3)_2$), 2.96 (s, 6H, -$N(CH_3)_2$); ^{13}C NMR (100 MHz, $CDCl_3$, 25°C), δ (ppm):155.80, 151.37, 140.11, 129.21, 107.96, 107.54, 104.09, 40.65, 36.48; HRMS *m/s* calc. for $C_{11}H_{17}N_3O$ + (H^+): 208.1444; found: 208.1451.

1,4-Bis-(3,3-dimethylureido)benzene (**D3**)

Following general procedure III with *p*-benzenediamine (260 mg, 2.40 mmol), Et_3N (800 µL 5.74 mmol), CH_2Cl_2 (5 mL), and dimethylcarbamoyl chloride (1 ml, 10.86 mmol), a white solid was obtained without purification. Yield = 230 mg (42%); R_f = 0.39 (MeOH/CH_2Cl_2 1:20); m.p. >290°C; ^{1}H NMR (400 MHz, DMSO-d6, 25°C), δ (ppm): 8.10 (s, 2H, -NHCO-), 7.29 (s, 4H,

H_{ar}), 2.91 (s, 12H, -CON(CH_3)$_2$); ^{13}C NMR (100 MHz, DMSO-d6, 25°C), δ (ppm):156.41, 135.36, 120.64, 36.65; HRMS *m/s* calc. for $C_{12}H_{18}N_4O_2$ + (H^+): 251.1503; found: 251.1500.

4.2. Biological evaluation

4.2.1. Cell Culture

3T3-L1 cells (ATCC) were grown and differentiated to mature adipocytes, as previously described, with minor modifications (Kershaw et al., 2006). Briefly 3 × 10^5 3T3-L1 cells were seeded in 35 mm dishes and maintained in Dulbecco's modified Eagle's medium containing high glucose concentrations (DMEM-HG; 4.5 g/L glucose) supplemented with 10% fetal bovine serum (FBS) (Gibco). Two days post-confluence (Day 0), cells were differentiated in DMEM-HG media containing 10% FBS, 10 µg/ml insulin from bovine pancreas, 0.4 µg/ml dexamethasone and 0.5 mM 3-Isobutyl-1-methylxanthine. After two days (Day 2), the media was changed to DMEM-HG supplemented with 10% FBS and 10 µg/ml insulin. At Day 4, the media was changed to DMEM-HG containing 10% FBS and 0.5 µg/ml insulin. After Day 6, cells were maintained in DMEM-HG containing 10% FBS. Experiments were performed with adipocytes at Day 8.

4.2.2. Lipolysis Assay

Adipocytes were washed twice with DMEM (1 g/L glucose) and pre-incubated with DMEM containing 2% (w/v) fatty acid-free bovine serum albumin (BSA) and 20 µM of indicated compound for 4 h. Lipolysis was stimulated by incubating cells with DMEM containing 2% FFA-BSA, 20 µM of indicated compound, and 5 µM of triacsin C (Sigma) in the presence of 2 µM isoproterenol for 1 h. Media aliquots were stored at -80ºC until analysis. Free glycerol and non-esterified fatty acids (NEFA) in the media were determined using colorimetric kit assays (free glycerol reagent from Sigma and HR Series NEFA-HR (2) kit from Wako Chemicals).

Cells were pelleted through centrifugation at 10,000 ×g for 10 min at 4°C, flash frozen in liquid N_2 and stored at -80°C until further use. 3T3-L1 cells were lysed in 100 µL of lysis buffer (20 mM Tris-HCl pH 7.5, 5 mM EDTA, 10 mM $Na_4P_2O_7$, 100 mM NaF, 1% NP-40) containing 2 mM sodium orthovanadate, 2 mM protease inhibitor cocktail (Sigma) and 100 µg/mL phosphatase inhibitor cocktail (Millipore). Protein concentrations in cell lysates were quantified colorimetrically using a bicinchoninic acid protein assay kit (Thermo Scientific) and BSA as standard.

4.3. Structure optimization and energy calculations

Calculations were performed using Gaussian 97 software. Structure optimization and energy calculations used DFT calculation at B3LYP/6-31G level of theory.

Statistical Analysis

Where necessary, statistical significance was determined using a One-way ANOVA with post-hoc Tukey HSD using Graphpad Prism software.

Acknowledgments

M.T. would like to acknowledge the contribution of the New Brunswick Innovation Foundation (NBIF), the Canadian Foundation for Innovation (CFI), and Université de Moncton. P.K. would like to acknowledge the contribution of the Natural Sciences and Engineering Research Council of Canada (NSERC).

References

[1] P. Morigny, M. Houssier, E. Mouisel, and D. Langin, Adipocyte lipolysis and insulin resistance, Biochimie. (2015), doi:10.1016/j.biochi.2015.10.024.

[2] B. B. Kahn and J. S. Flier, Obesity and insulin resistance, J. Clin. Invest. 106 (2000), 473-481

[3] R. A. DeFronzo, Insulin resistance, lipotoxicity, type 2 diabetes and atherosclerosis: the missing links. The Claude Bernard Lecture 2009, Diabetologia, vol. 53 (2010), 1270–1287

[4] C. M. Kusminski, S. Shetty, L. Orci, R. H. Unger, and P. E. Scherer, Diabetes and apoptosis: lipotoxicity, Apoptosis. 14 (2009), 1484-1495

[5] K. L. Kliewer, J.-Y. Ke, M. Tian, R. M. Cole, R. R. Andridge, and M. A. Belury, Adipose tissue lipolysis and energy metabolism in early cancer cachexia in mice, Cancer Biol. Ther. 16 (2015), 886-897.

[6] S. K. Das, S. Eder, S. Schauer, C. Diwoky, H. Temmel, B. Guertl, G. Gorkiewicz, K. P. Tamilarasan, P. Kumari, M. Trauner, R. Zimmermann, P. Vesely, G. Haemmerle, R. Zechner, and G. Hoefler, Adipose Triglyceride Lipase Contributes to Cancer-Associated Cachexia, Science. 333 (2011), 233-238.

[7] A. Lass, R. Zimmermann, M. Oberer, and R. Zechner, Lipolysis – A highly regulated multi-enzyme complex mediates the catabolism of cellular fat stores, Prog. Lipid Res. 50 (2011), 14-27.

[8] R. Zechner, P. C. Kienesberger, G. Haemmerle, R. Zimmermann, and A. Lass, Adipose triglyceride lipase and the lipolytic catabolism of cellular fat stores, J. Lipid Res. 50 (2009), 3-21.

[9] R. Zimmermann, J. G. Strauss, G. Haemmerle, G. Schoiswohl, R. Birner-Gruenberger, M. Riederer, A. Lass, G. Neuberger, F. Eisenhaber, A. Hermetter, and R. Zechner, Fat Mobilization in Adipose Tissue Is Promoted by Adipose Triglyceride Lipase, Science. 306 (2004), 1383-1386.

[10] N. Mayer, M. Schweiger, M. Romauch, G. F. Grabner, T. O. Eichmann, E. Fuchs, J. Ivkovic, C. Heier, I. Mrak, A. Lass, G. Höfler, C. Fledelius, R. Zechner, R. Zimmermann, and R.

Breinbauer, Development of small-molecule inhibitors targeting adipose triglyceride lipase, Nat. Chem. Biol. 9 (2013), 785-787.

[11] I. K. Cerk, B. Salzburger, A. Boeszoermenyi, C. Heier, C. Pillip, M. Romauch, M. Schweiger, I. Cornaciu, A. Lass, R. Zimmermann, R. Zechner, and M. Oberer, A Peptide Derived from G0/G1 Switch Gene 2 Acts as Noncompetitive Inhibitor of Adipose Triglyceride Lipase, J. Biol. Chem. 289 (2014), 32559-32570.

[12] N. Mayer, M. Schweiger, M.-C. Melcher, C. Fledelius, R. Zechner, R. Zimmermann, and R. Breinbauer, Structure–activity studies in the development of a hydrazone based inhibitor of adipose-triglyceride lipase (ATGL), Bioorg. Med. Chem. 23 (2015), 2904-2916.

[13] P. C. Kienesberger, D. Lee, T. Pulinilkunnil, D. S. Brenner, L. Cai, C. Magnes, H. C. Koefeler, I. E. Streith, G. N. Rechberger, G. Haemmerle, J. S. Flier, R. Zechner, Y.-B. Kim, and E. E. Kershaw, Adipose Triglyceride Lipase Deficiency Causes Tissue-specific Changes in Insulin Signaling, J. Biol. Chem. 284 (2009), 30218-30229.

[14] A. J. Hoy, C. R. Bruce, S. M. Turpin, A. J. Morris, M. A. Febbraio, and M. J. Watt, Adipose Triglyceride Lipase-Null Mice Are Resistant to High-Fat Diet–Induced Insulin Resistance Despite Reduced Energy Expenditure and Ectopic Lipid Accumulation, Endocrinology. 152 (2011), 48-58.

[15] G. Haemmerle, T. Moustafa, G. Woelkart, S. Büttner, A. Schmidt, T. van de Weijer, M. Hesselink, D. Jaeger, P. C. Kienesberger, K. Zierler, R. Schreiber, T. Eichmann, D. Kolb, P. Kotzbeck, M. Schweiger, M. Kumari, S. Eder, G. Schoiswohl, N. Wongsiriroj, N. M. Pollak, F. P. W. Radner, K. Preiss-Landl, T. Kolbe, T. Rülicke, B. Pieske, M. Trauner, A. Lass, R. Zimmermann, G. Hoefler, S. Cinti, E. E. Kershaw, P. Schrauwen, F. Madeo, B. Mayer, and R. Zechner, ATGL-mediated fat catabolism regulates cardiac mitochondrial function via PPAR-α and PGC-1, Nat. Med. 17 (2011), 1076-1085.

[16] P. C. Kienesberger, T. Pulinilkunnil, J. Nagendran, M. E. Young, J. G. Bogner-Strauss, H. Hackl, R. Khadour, E. Heydari, G. Haemmerle, R. Zechner, E. E. Kershaw, and J. R. B. Dyck, Early structural and metabolic cardiac remodelling in response to inducible adipose triglyceride lipase ablation, Cardiovasc. Res. 99 (2011), 442-451.

[17] K. Hirano, Y. Ikeda, N. Zaima, Y. Sakata, and G. Matsumiya, Triglyceride deposit cardiomyovasculopathy, N. Engl. J. Med. 359 (2008), 2396-2398.

[18] A. Suzuki, Cross-coupling reactions via organoboranes, J. Organomet. Chem. 653 (2002), 83-90.

[19] G. Cheng and M. Luo, Homocoupling of Arylboronic Acids Catalyzed by CuCl in Air at Room Temperature, Eur. J. Org. Chem. 2011 (2011), 2519-2523.

[20] E. J. Lien, Z. R. Guo, R. L. Li, and C. T. Su, Use of dipole moment as a parameter in drug-receptor interaction and quantitative structure-activity relationship studies, J. Pharm. Sci. 71 (1982), 641-655.

Research highlight

► Novel Atglistatin closely related analogues were synthesized.

► Structure-activity relationships were established based on adipose triglyceride lipase inhibition.

►The meta-relationship of the substituents was critial for adipose triglyceride lipase inhibition.